World Academy of Science, Engineering and Technology
International Journal of Materials and Metallurgical Engineering
Vol:12, No:10, 2018

Micromechanical Modeling of Fiber-Matrix Debonding in Unidirectional Composites

M. Palizvan, M. T. Abadi, M. H. Sadr

***Abstract*—**Due to variations in damage mechanisms in the microscale, the behavior of fiber-reinforced composites is nonlinear and difficult to model. To make use of computational advantages, homogenization method is applied to the micro-scale model in order to minimize the cost at the expense of detail of local microscale phenomena. In this paper, the effective stiffness is calculated using the homogenization of nonlinear behavior of a composite representative volume element (RVE) containing fiber-matrix debonding. The damage modes for the RVE are considered by using cohesive elements and contacts for the cohesive behavior of the interface between fiber and matrix. To predict more realistic responses of composite materials, different random distributions of fibers are proposed besides square and hexagonal arrays. It was shown that in some cases, there is quite different damage behavior in different fiber distributions. A comprehensive comparison has been made between different graphs.

***Keywords*—**Homogenization, cohesive zone model, fiber-matrix debonding, RVE.

I. Introduction

SINCE fiber-reinforced composite materials have strong mechanical performance (high stiffness and strength to the weight, higher fatigue life, corrosion resistance, and a reasonable production cost), they have been applied in a wide range of structural applications, especially in the aerospace industry. The desired performance of a fibrous composite material could be achieved by choosing different constituents, different volume fractions, and various matrix-fiber arrangements. In order to use any sort of composite materials, it is certainly essential to understand their mechanical properties at different scales. However, the mechanical response of composite materials may be affected by several damage mechanisms in which the fiber matrix debonding and matrix cracking are of the primary damage modes. Although the initiation and propagation of these damage modes will not cause the collapse of the structure directly; however, they instantly will decrease the strength of the damaged layer a bit.

Note that the lack of an integrated computational framework for predicting the mechanical response of fiber-reinforced composite materials could lead to a huge number of experimental tests for the reliable design of structural components. An alternative approach is to employ a RVE [1] to synthesize realistic models of the fiber-reinforced composite microstructure. RVE is a statistical representation of typical material properties. RVE is widely used in nowadays mechanics, and many authors were using the concept of RVE for theoretical, numerical, and experimental purposes [1]-[9].

Many researchers have studied the impacts of the probable damage modes in the response of composite materials with special consideration on fiber-matrix debonding based on micromechanics of RVEs. Mishnaevsky and Brondsted [2] have used a cohesive damage modeling approach to investigate the mechanical behavior and damage evolution of glass fiber-reinforced composites. The authors have developed a code for automatic generation of micromechanical unit cells of composites with damageable elements. The statistical variability of fiber strength, fiber-matrix interface debonding, and other features have been embedded into the code. Numerical experiments have been conducted using the generated unit cell models to investigate different fiber packing geometries.

A Cohesive Zone Model (CZM) was proposed in [3] to describe the fracture of adhesively bonded polymer-matrix composites. More recently, an inverse procedure to identify the mode I cohesive parameters of bonded interfaces is proposed in [4]. It bears emphasis that some of the fracture parameters can be obtained using purely experimental based approaches or J-integral related methods.

Melro et al. [5], [6] presented the application of a constitutive damage model for an epoxy matrix on micromechanical analyses of polymer composite materials. Different RVEs with periodic boundary were generated with a random distribution of fibers. The focus was given to the influence of the interface between fiber and matrix, as well as to the importance of the epoxy matrix, on the strength properties of the composite, damage initiation and propagation under different loading conditions. The impact of the interface properties (interface strength and toughness) on the tensile deformation was studied in a model composite made of a random distribution of stiff spherical particles embedded in a ductile matrix by Segurado and Llorica [7]. The composite behavior was simulated through the finite element analysis of an RVE of the composite microstructure, and interface decohesion was included by means of interface elements whose response was governed by a cohesive crack model. The ability to use the changes in elastic stiffness or in volumetric strain to monitor damage during deformation was determined and simple models of continuum damage mechanics based on these parameters failed to predict the composite flow stress in the presence of interface decohesion.

M. Palizvan is with the Aerospace Research Institute, Tehran, Iran (corresponding author, e-mail: palizvan@sun.ari.ac.ir).

M. T. Abadi is with the Department of Aerospace Engineering (Structural design), Aerospace Research Institute, Tehran, Iran (e-mail: Abadi@ari.ac.ir).

M. H. Sadr is with the Aerospace Engineering Department, Amirkabir University of Technology, Tehran, Iran (e-mail: Sadr@aut.ac.ir).

II. Modelling the Cohesive Zone

Fiber-matrix debonding is one of the most common types of damage in micromechanical scale in laminated fiber reinforced composites due to their relatively weak interlaminar strengths. Fiber matrix debonding may significantly affect the composite stiffness and strength. It may arise in such structures under various circumstances, but most of the time when subject to transverse loadings.

The CZM approach has emerged as a powerful analytical tool for nonlinear fracture processes. CZMs have particularly been used to analyze composite debonding problems. However, in many studies, they had the assumption of the existence of initial defects or cracks and could not be applied directly without initial debonding. But, this limitation becomes very challenging or even impossible when a random distribution of fibers is utilized for an RVE with hundreds of fibers. In many applications, stress-based methods have to be used to predict the initiation of debonding, following which fracture mechanics can be applied to describe the propagation of existing debonding, see for example [6], [8], [9].

A micromechanical model for composite microstructures undergoing fiber-matrix interfacial debonding has been developed in Swaminathan et al. study [10]. In this model, the fiber-matrix interface behavior is modeled by a nonlinear CZM with bilinear traction-displacement relations in both normal and tangential directions. Bilinear CZMs show an acceptable agreement with experiments for composite materials described in [11], [12]. The interface is modeled by a set of cohesive springs that are tied to the fiber and the matrix at both sides. By increasing displacement, the traction across the interface increases to a maximum value, then decreases with further displacement increase, and at the end, vanishes indicating failure of the spring.

III. Generation of Random RVEs

The introduction of randomness to the fiber positions in the microstructure is desirable for a variety of reasons. It results in a more realistic microstructure. Randomness leads to fibers in very close proximity to one another, which gives rise to high-stress concentrations. These concentrations will strongly influence extreme-based mechanisms such as failure and plasticity. The introduction of randomness can also be useful for the characterization of uncertainty in composite properties. The use of random microstructures to predict the behavior of composites is not new.

Firstly, in order to analyze the mechanical properties of composites, considering their microstructure details, an appropriate RVE model of composites should be defined. In this section, the procedure is illustrated for the automatic generation of RVE models with a random distribution of fibers. A micrograph of an actual lamina illustrates that physical lamina does not exhibit a uniform distribution of fibers but rather have some random distribution. As a result, this work aims to model the lamina microstructure more accurately by introducing randomness into the arrangement of fibers. These models could be used for long fiber reinforced composite micro-mechanical analysis. The program code is developed in MATLAB language. Then, one can use the files to generate RVE and execute subsequence numeral analysis conveniently.

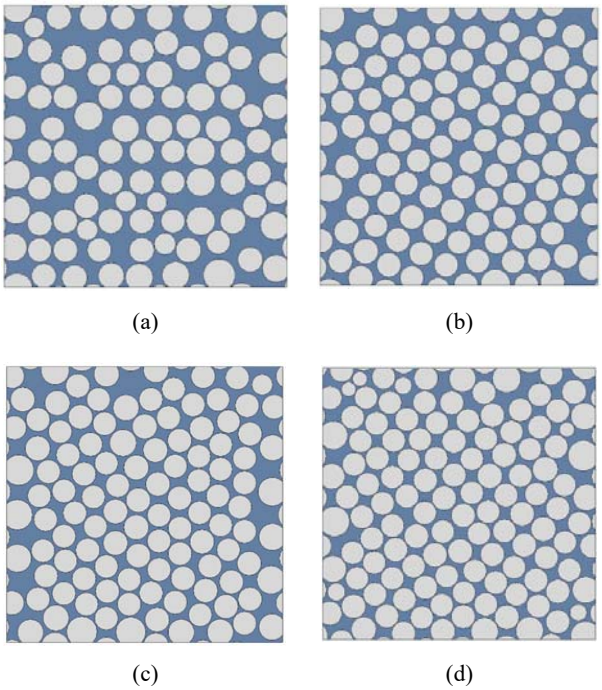

Fig. 1 Random fiber distribution in RVE for different fiber volume fraction, (a) 60%, (b) 65%, (c) 70%, (d) 75%

IV. Micromechanical Properties Evaluation

Various finite element analyses with different fiber volume fraction RVEs are generated. For the elastic material behavior section, several papers are validated with different material behavior, RVE size, fiber size, etc.

A. Finite Element Analysis

Finite element (FE) analysis was carried out using ABAQUS [13] under plane strain condition. In the ABAQUS model, both the matrix and the fibers were meshed using free meshing technique with quad-dominated element shapes. The two-dimensional 4-node bilinear plane strain quadrilateral elements (CPE4) were chosen to mesh the fiber and the matrix. There was also a relatively small amount of 3-node linear plane strain triangle elements (CPE3) due to the free meshing technique used. Since each model has about 500 fibers, it is difficult and time-consuming to generate each RVE manually. Therefore, python scripts have been written to generate and distribute fibers in the FE models of the RVEs in ABAQUS [13].

B. Periodic Boundary Conditions

The importance of periodic boundary conditions in the world of micromechanical analysis has been demonstrated by several authors [14]-[16]. The present subsection is devoted to the derivation of the equations to be applied to the RVE's mesh in order to implement this type of boundary conditions.

Periodic boundary conditions force such a deformation on the volume element that the displacement of one of the nodes belonging to one edge must be related to the displacement of the corresponding node in the opposite edge. Fig. 2 exemplifies the final result.

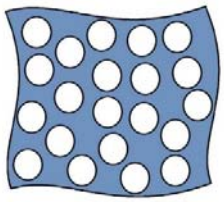

Fig. 2 Periodic boundary conditions

Barbero [16] provides a set of equations that allow the application of periodic boundary conditions in a RVE. All equations must be applied to opposite nodes on the faces, edges, and vertices of the RVE. Not only the degrees of freedom of these nodes are variables in these equations but also the far-field applied strains. Depending on which position the nodes are – edges or vertices – a different set of equations must be applied to its degrees of freedom. These equations can be incorporated in a FE analysis by using linear multi-point constraints.

V. Analysis and Results

The current section is dedicated to the analysis of debonding damage behavior of long fiber composite materials at micro-scale. To study the trends thoroughly, different RVEs configurations implemented. Two types of regular fiber distribution in the matrix are investigated, the square and hexagonal array fiber distributions; the third form is a random distribution. The results are presented for 20, 40, and 60 percent of fiber volume fractions.

Throughout the studies, a square of 100 by 100 micrometers and a fiber radius of 5 micrometers are assumed and material properties are taken from Legard et al. [17]. Material models are assumed to be linear elastic for matrix and fibers, and their interaction is modeled using cohesive elements. Each case is studied by mean of Von-Mises stress distribution contour investigations as well as deformation description and stress-strain and damage propagation behavior. The analyses are continued by debonding study as mean of damage indicator and its effect on Poisson's ratio of RVEs.

A. Square Array Distribution

The RVEs with the square array distribution of the fibers are analyses under uniaxial tension, the Von-Mises stress contour for RVEs with 20%, 40% and 60% fiber volume fractions are shown in Fig. 3. The deformation of RVEs after loading ($\varepsilon_{xx} = 0.02$) and the distribution of interfaces that included fiber-matrix debonding are different in various fiber volume fractions.

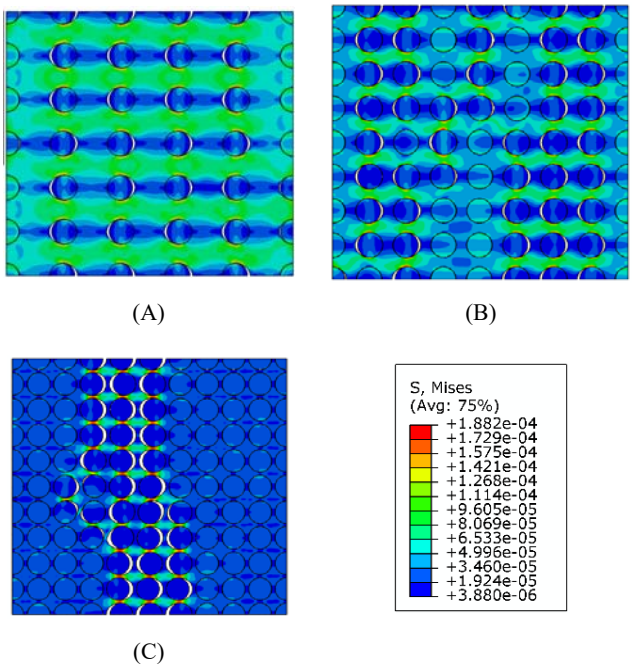

Fig. 3 Von-Mises stress contour for RVEs with 20%, 40%, and 60% fiber volume fractions and square array fiber distributions (Stress in $Pa \times 10^{-12}$

In the RVE with 20% fiber volume fraction, Fig. 3 (A), almost all the fibers experienced the fiber-matrix debonding. In the other words, the damage has spread all over the RVE. However, in RVE with 40% fiber volume fraction and square array fiber distribution, Fig. 3 (B), the only fibers that are in the two left and right strips are debonded and the fibers in the middle of the RVE have remained perfectly without damage. This phenomenon is observed in RVE with 60% fiber volume fraction in a different scheme, see Fig. 3 (A). Only a narrow strip of fibers in the middle the RVE contains debonding in their interfaces, and the rest of the fibers remain completely undamaged.

By increasing the fiber volume fraction and by keeping the radius constant, the number of fibers within the RVE increases obviously. And when the loading is done, the fibers inside the RVE are debonded and with every fiber-matrix debonding, specific amount of energy is dissipated. In the low fiber volume fraction RVEs (in this case 20%), all fibers must be debonded to provide the dissipated energy. However, with increasing fiber volume fraction, a lower percentage of fibers is needed to provide it. It should be noted that due to the different amount of damage developed in different RVEs, after loading ($\varepsilon_{xx} = 0.02$), the amount of dissipated energy is varied.

This phenomenon can be described in another way. The RVEs with low fiber volume fraction has fewer fibers. So, the distances between the fibers are more than the distances between the fibers with higher fiber volume fraction. In this case, there is a more uniform distribution of stress in the RVE even when some debonding occurred. This uniform distribution of stress is caused by the elastic properties of the

matrix and the adequate distance of the fibers from each other. However, in the RVE with more fiber volume fraction (40% and 60%), the fibers must place with less distance so there is a narrower matrix band between them. In another word, in the same area, more fibers should be placed. The damage will have a greater impact on the distribution of the stress of the neighboring fibers when the fibers are close to each other. For this reason, when the first fiber matrix debonding occurred in the fibers' interaction, the following stress concentration will cause the next debonding in the neighboring fibers. And that's why in the high fiber volume fraction RVEs, the damage is clustered and occurs only in certain sections in the RVE.

The stress-strain relations for RVEs with square array fiber distribution are shown in Fig. 4 (A), it can be understood that damage in lower fiber volume fraction is occurred in a larger strain in compare by higher ones. As it can be seen in Fig. 4 (A), for RVE with square array fiber distribution and 20%, 40% and 60% fiber volume fractions, damage initiates in strain $\varepsilon = 0.0087$, 0.0065 and 0.0046, respectively.

Damage initiates earlier in RVE with 60% fiber volume fraction because the fibers are very close to each other which is lead to more stress concentrations. On the other hand, according to Fig. 4 (A), besides the earlier damage initiation, the stiffness loss is more and about 15 MPa. The remarkable point is that although the RVE with 20% fiber fraction has a lower stiffness, its strength is more than the other RVEs. This can be explained by the fact that due to the earlier debondings initiate in the RVE with 60% volume fraction and the subsequent debondings caused by stress concentrations, the RVE with more fiber volume fractions show lower stress strength.

At all stages of loading from the first debonding, the amount of damage for RVE with 60% volume fraction is higher than the others and ultimately reaches D=0.73 in strain $\varepsilon = 0.02$. This is while for the other two RVEs, damage reaches D=0.65 and 0.42 for 40% and 20% volume fractions, respectively.

The variation of the Poisson's ratio to the initial value is shown in Fig. 4 (B). Since damage is zero at the beginning of loading, the effective material properties have still remained in the elastic regime so in the absence of damage, the Poisson's ratio stayed unchanged. By the first damage initiation, the Poisson's ratio starts to decrease uniformly and with different slopes in all three RVEs. Since the most damage is made in RVE with 60% fiber volume fraction, the Poisson's ratio drop is larger than the other RVEs.

B. Hexagonal Array Distribution

To have a better perspective of the behavior of RVE with regular fiber arrangement containing fiber-matrix debonding, three RVEs with 20%, 40%, and 60% fiber volume fraction considered with hexagonal array fiber distributions in this section. The Von-Mises stress contours at strain $\varepsilon_{xx} = 0.02$ for these RVEs are shown in Fig. 5.

Just like the previous section, square array fiber distribution, the debondings are spread all over the RVE with 20% fiber volume fraction. This means that the debonding is almost happened for all the fibers, see Fig. 5 (A).

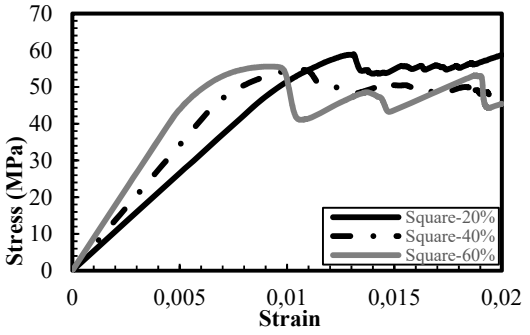

(A)

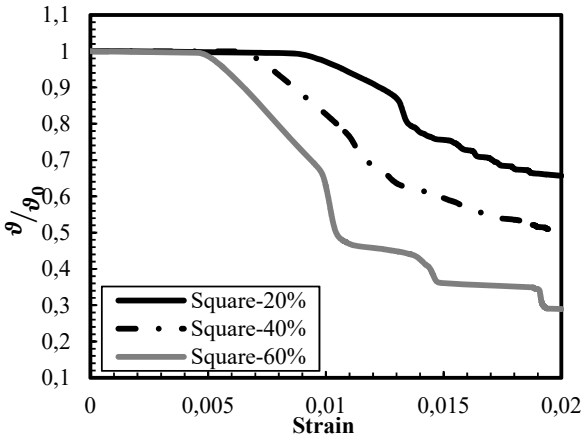

(B)

Fig. 4 (A) stress-strain relation and (B) Poisson's ratio variation-strain relation obtained from modeling three RVEs with square array distributions with 20%, 40%, and 60% fiber volume fractions under uniaxial loading

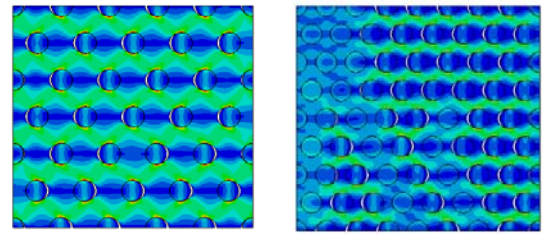

(A) (B)

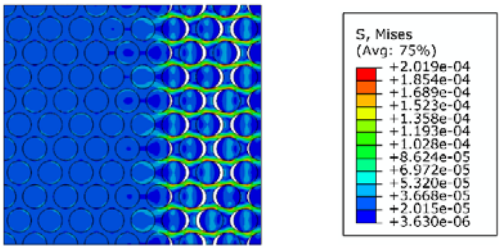

(C)

Fig. 5 Von-Mises stress contour for RVEs with 20%, 40% and 60% fiber volume fractions and hexagonal array fiber distributions (Stress in $Pa \times 10^{-12}$

Once again, the fibers debonded in two groups in two side of the RVE for 40% volume fraction shown in Fig. 5 (B). This two groups of fibers contain fiber-matrix debonding in their interactions are asymmetric in hexagonal array distribution. However, we can see almost a symmetric scheme of debonding in 40% fiber volume fraction with square array distribution.

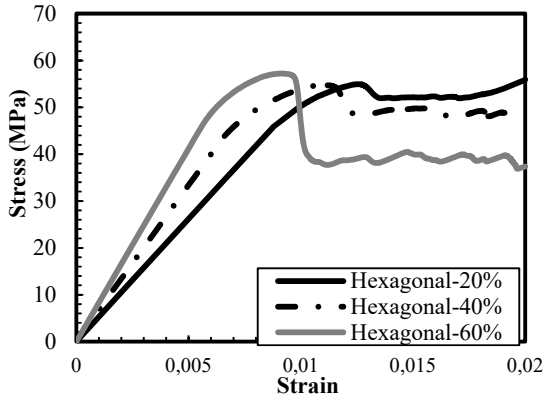

(A)

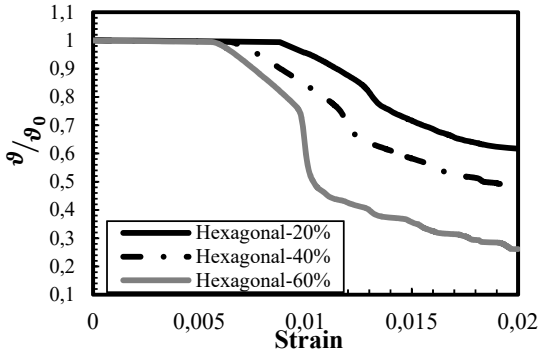

(B)

Fig. 6 (A) stress-strain relation and (B) Poisson's ratio variation-strain relation obtained from modeling three RVEs with hexagonal array distributions for 20%, 40% and 60% fiber volume fractions under uniaxial loading

Although as we expected, the debonding for 60% fiber volume fraction happens in a narrow strip of the fibers unlike the square array fiber distribution, the strip of debonded fibers is located at the vicinity of loading edge.

Stress-strain curves are illustrated in Fig. 6 (A) for three different fiber volume fractions in RVEs with hexagonal fiber distribution. The RVE with 60% fiber volume fraction experiences fiber-matrix debonding in strain $\varepsilon = 0.095$, which results in a 20 MPa drop in its strength. Besides this early damage initiation, its ultimate strength is still more than two other fiber volume fractions. RVEs with 20% and 40% fiber volume fractions are decreased about 5 MPa in $\varepsilon = 0.0125$ and $\varepsilon = 0.0115$ in their stress curves, respectively.

Fig. 6 (B) shows how the Poisson ratio changes. It can be concluded the with the increase of damage parameter, we have degradation in Poisson's ratio. There is about 75, 50, and 35 percent reduction for the RVE with 60, 40, and 20 percent fiber volume fraction, respectively.

C. Random Distribution

In the previous two sections, the damage behavior of RVEs with regular fiber distribution (square and hexagonal arrays) has been studied. While in fact the distributions of fibers in real composites are not regular, this can be an unrealistic assumption. In this section, RVEs with random fiber distribution have been modeled to have a more realistic damage initiation and propagation. Three random fiber distributions are assumed with 20%, 40%, and 60% fiber volume fraction, shown in Fig. 7.

Unlike the previous sections that almost all the fibers experienced the fiber matrix debonding in the 20% fiber volume fraction, in the random arrangement, a fewer number of fibers debonded (Fig. 7 (A)). It should be noted that the damage behavior of RVE has a strong dependency on the fibers locations in the random fiber distributions. And the debonding always develops in places where the most tension is applied to the cohesive interface. In this RVE, Fig. 7 (A), the location of the debonding could be predicted in advance, since the first debonding occurs at the place where the maximum tensile force is applied to the interface between the fiber and the matrix, or in the other words, the least load is tolerated at that cross-section of the matrix. This will occur at the cross-sectional stage where the matrix has the lowest width. It can be seen that seven fibers are located in the same vertical direction where the first debonding happened. There is the lowest width of the matrix in this vertical cross-section between the different sections in this RVE (Fig. 7 (A)).

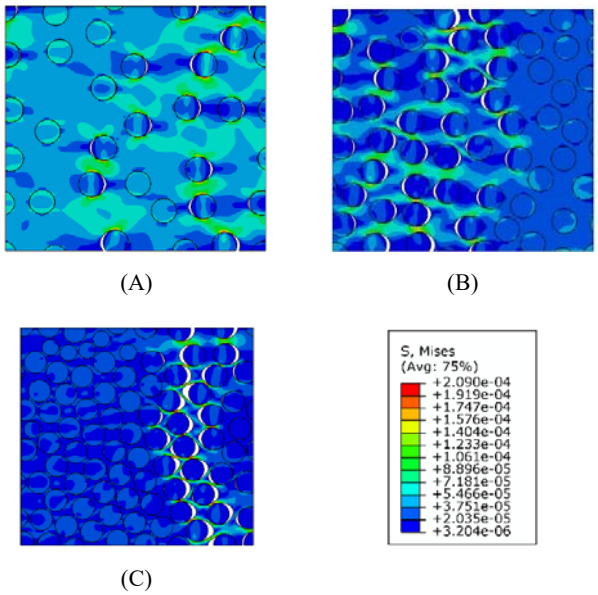

(A) (B)

(C)

Fig. 7 Von-Mises stress contour for RVEs with 20%, 40%, and 60% fiber volume fractions and square array fiber distribution (Stress in $Pa \times 10^{-12}$)

The deformation of the RVE with random fiber distribution

and 40% fiber volume fraction by $\varepsilon = 0.02$ is shown in Fig. 7 (B). The debonding interfaces are located on the left side of the RVE, while in the two previous section (square and hexagonal distributions), in this fiber volume fraction, the debonding interfaces occurred on both sides of the RVEs.

Contrary to two RVEs with 20% and 40% fiber volume fractions that have a different distribution of damage regarding to the regular fiber distributions RVEs, in RVE with 60% fiber volume fraction (Fig. 7 (C)), the deformation and distribution pattern of the damage is very similar to distributions of damage in square and hexagonal fiber arrays. So, a narrow strip of fibers from the top to the bottom are debonded.

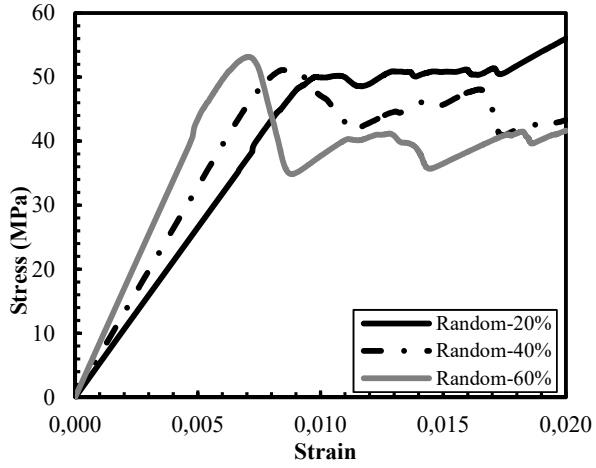

(A)

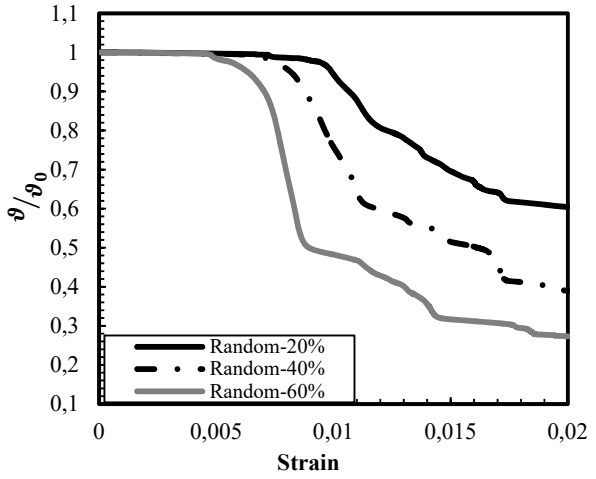

(B)

Fig. 8 (A) stress-strain relation and (B) Poisson's ratio variation-strain relation obtained from modeling three RVEs with random fiber distributions for 20%, 40% and 60% fiber volume fractions under uniaxial loading

D.RVEs with 60% Fiber Volume Fractions and Different Fiber Distributions

As can be expected, by the change in fiber fraction, the RVEs behavior changes considerably. As fibers close in, damage initiation and propagation concentrate in the same spots. In Fig. 9 (A), it is illustrated that randomly distributed RVE having 60 percent fiber fraction undergoes the decrease in stiffness sooner than ordered models for about 4 MPa less maximum stress; as observed in 20 and 40 percent fiber fraction RVEs. Introductory loss of stiffness in all three configurations is about 20 MPa. The observed decrease is gradual at hexagonal formation rather than a triple steep reduction in the squared and random distribution of fibers. Finally, at 3 percent strain, bearing stress in squared order has the highest, while the hexagonal and fiber distribution model has the lowest stress-bearing capacity.

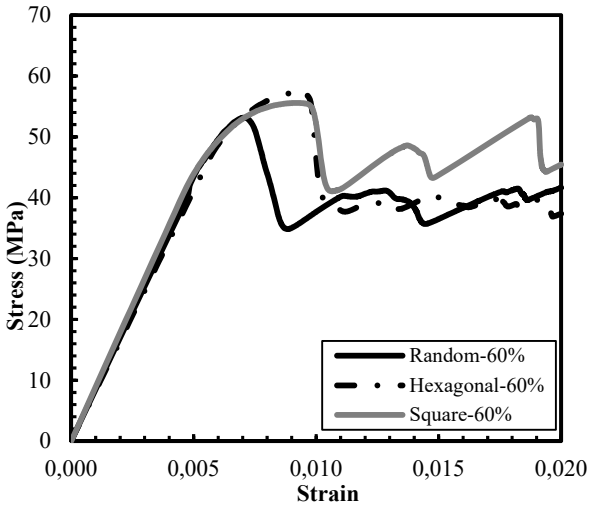

(A)

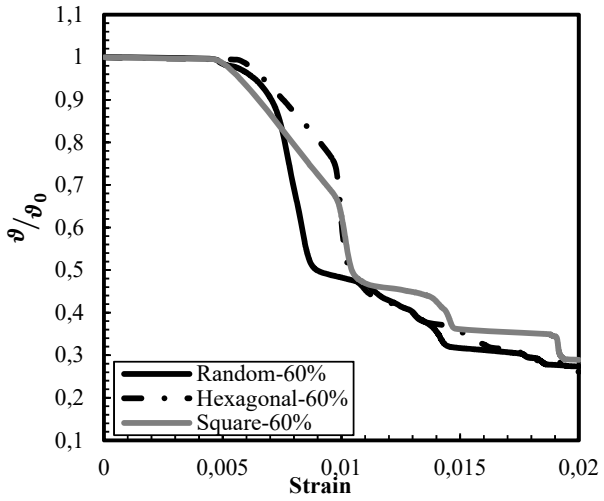

(B)

Fig. 9 (A) stress-strain relation and (B) Poisson's ratio variation-strain relation obtained from modeling three RVEs with 60% random fiber volume fraction for square array, hexagonal array and random distributions under uniaxial loading

VI. Conclusion

A micromechanical study to predict the mechanism of debonding of a fibrous composite material under transverse tension to the fibers has been carried out. Several RVEs with

regular (square and hexagonal arrays) and random fiber distributions have been studied by means of the FE method, considering an interface crack between the fiber and the matrix.

Through the use of RVEs, we demonstrate the influence of interphases and interfacial debonding on the global response of fibrous reinforced composites. We capture the interfacial debonding behavior of the fibers, at large strains, using cohesive elements. It has been shown that interphases significantly alter the macroscopic constitutive response of these composite materials. This study indicates that the proposed computational framework is able to provide an explanation for the varied macroscopic response of fiber reinforced composite. Because of the challenges associated with experimentally obtaining the necessary measurements of material properties, a computational framework, such as the one presented in this paper. In summary, this paper has been able to clearly demonstrate the significance of interphases and interfacial debonding on the macroscopic constitutive response of fibrous reinforced composites.

Ultimately, the goal would be to use this investigation as an introduction of part two in which both fiber-matrix debonding at fiber interface and matrix cracks are considered at the same time.

REFERENCES

[1] Xu, Hongyi, et al. Descriptor-based methodology for statistical characterization and 3D reconstruction of microstructural materials. Computational Materials Science, 2014, 85: 206-216.
[2] Mishnaevsky JR, Leon; Brøndsted, Povl. Micromechanisms of damage in unidirectional fiber reinforced composites: 3D computational analysis. Composites Science and Technology, 2009, 69.7-8: 1036-1044.
[3] Li, S., et al. Use of mode-I cohesive-zone models to describe the fracture of an adhesively-bonded polymer-matrix composite. Composites Science and Technology, 2005, 65.2: 281-293.
[4] Valoroso, Nunziante, et al. Identification of mode-I cohesive parameters for bonded interfaces based on DCB test. Engineering Fracture Mechanics, 2013, 104: 56-79.
[5] Melro, A. R., et al. Micromechanical analysis of polymer composites reinforced by unidirectional fibres: Part I–Constitutive modelling. International Journal of Solids and Structures, 2013, 50.11-12: 1897-1905.
[6] Melro, A. R., et al. Micromechanical analysis of polymer composites reinforced by unidirectional fibres: Part II–micromechanical analyses. International Journal of Solids and Structures, 2013, 50.11-12: 1906-1915.
[7] Segurado, Javier; Llorca, Javier. A computational micromechanics study of the effect of interface decohesion on the mechanical behavior of composites. Acta materialia, 2005, 53.18: 4931-4942.
[8] Totry, Essam, et al. Effect of fiber, matrix and interface properties on the in-plane shear deformation of carbon-fiber reinforced composites. Composites Science and Technology, 2010, 70.6: 970-980.
[9] O'dwyer, D. J.; O'dowd, N. P.; Mccarthy, C. T. Numerical micromechanical investigation of interfacial strength parameters in a carbon fibre composite material. Journal of Composite Materials, 2014, 48.6: 749-760.
[10] Swaminathan, Shriram; Pagano, N. J.; Ghosh, Somnath. Analysis of interfacial debonding in three-dimensional composite microstructures. Journal of engineering materials and technology, 2006, 128.1: 96-106.
[11] Li, Shanhu; Ghosh, Somnath. Debonding in composite microstructures with morphological variations. International Journal of computational methods, 2004, 1.01: 121-149.
[12] Chandra, N., et al. Some issues in the application of cohesive zone models for metal–ceramic interfaces. International Journal of Solids and Structures, 2002, 39.10: 2827-2855.
[13] ABAQUS, Inc. ABAQUS theory and standard user's manual. 2003.
[14] Xia, Zihui; Zhang, Yunfa; Ellyin, Fernand. A unified periodical boundary conditions for representative volume elements of composites and applications. International Journal of Solids and Structures, 2003, 40.8: 1907-1921.
[15] Nguyen, V.-D., et al. Imposing periodic boundary condition on arbitrary meshes by polynomial interpolation. Computational Materials Science, 2012, 55: 390-406.
[16] Barbero, Ever J. Finite element analysis of composite materials using AbaqusTM. CRC press, 2013.
[17] Legarth, Brian Nyvang; Yang, Qingda. Micromechanical analyses of debonding and matrix cracking in dual-phase materials. Journal of Applied Mechanics, 2016, 83.5: 051006.